Positron emission tomography imaging of dopamine D2 receptors using a highly selective radiolabeled D2 receptor partial agonist

Jinbin Xu[1], **Suwanna Vangveravong**[1], **Shihong Li**[1], **Jinda Fan**[1], **Lynne A. Jones**[1], **Jinquan Cui**[1], **Ruike Wang**[1], **Zhude Tu**[1], **Wenhua Chu**[1], **Joel S. Perlmutter**[1], and **Robert H. Mach**[1,2,3]

[1]Department of Radiology, Washington University School of Medicine, 510 S. Kingshighway Blvd., St. Louis, MO 63110, USA

[2]Department of Cell Biology and Physiology, Washington University School of Medicine, 510 S. Kingshighway Blvd., St. Louis, MO 63110, USA

[3]Department of Biochemistry and Molecular Biophysics, Washington University School of Medicine, 510 S. Kingshighway Blvd., St. Louis, MO 63110, USA

Abstract

A series of microPET imaging studies were conducted in anesthetized rhesus monkeys using the dopamine D_2-selective partial agonist, [^{11}C]**SV-III-130**. There was a high uptake in regions of brain known to express a high density of D_2 receptors under baseline conditions. Rapid displacement in the caudate and putamen, but not in the cerebellum, was observed after injection of the dopamine $D_{2/3}$ receptor nonselective ligand $S(−)$-eticlopride at a low dosage (0.025 mg/kg/ i.v.); no obvious displacement in the caudate, putamen and cerebellum was observed after the treatment with a dopamine D_3 receptor selective ligand **WC-34** (0.1 mg/kg/i.v.). Pretreatment with lorazepam (1 mg/kg, i.v. 30 min) to reduce endogenous dopamine prior to tracer injection resulted in unchanged binding potential (BP) values, a measure of D_2 receptor binding *in vivo*, in the caudate and putamen. D-amphetamine challenge studies indicate that there is a significant displacement of [^{11}C]**SV-III-130** by d-amphetamine-induced increases in synaptic dopamine levels.

Keywords

Dopamine; Dopamine D_2 receptors; Positron Emission Tomography

INTRODUCTION

Based on genetic and pharmacological studies, dopamine receptors are classified as the D_1-like (D_1 and D_5 receptor subtypes) and the D_2-like (D_2, D_3 and D_4 receptor subtypes). Agonist stimulation of D_1-like receptors activate adenylyl cyclase via coupling to the $G_{alpha(S)}/G_{alpha(olf)}$ class of G proteins (Herve et al., 2001). Stimulation of the D_2-like

receptors leads to the inhibition of adenylyl cyclase activity via coupling with the G_i/G_o class of G proteins (Sibley and Monsma, 1992, Sealfon and Olanow, 2000, Vallone et al., 2000). Dopamine receptor subtypes regulate dopaminergic circuits in a variety of neurological and neuropsychiatric disorders, including Parkinson's disease, dystonia and schizophrenia (Lee et al., 1978, Missale et al., 1998, Jardemark et al., 2002, Nieoullon, 2002, Kapur and Mamo, 2003, Korczyn, 2003, Luedtke and Mach, 2003, Karimi et al., 2011). In addition, activation of the dopaminergic pathways may mediate the reinforcing effects of pyschostimulants, including cocaine and amphetamines (Uhl et al., 1998, Nader et al., 1999, Volkow et al., 2002). Dopamine receptors were also involved in the sleep deprivation-induced remodeling of dopamine circuits (Lim et al., 2011).

Positron emission tomography (PET) is an *in vivo* imaging technique which is capable of providing measures of receptor density in the living human brain. To date numerous PET imaging studies have been reported using carbon-11 and fluorine-18 labeled radiotracers such as [^{11}C]raclopride, [^{11}C]fallypride, [^{18}F]fallypride, and [^{11}C]FLB 457 (Yokoi et al., 2002, Buchsbaum et al., 2006, Cselenyi et al., 2006, Volkow et al., 2008, Narendran et al., 2009, Vandehey et al., 2010). However, these radiotracers are nonselective antagonists at both D_2 and D_3 receptors; consequently, the measure of dopamine receptor density, commonly referred to as the "binding potential", is typically reported as the $D_{2/3}$ receptor binding potential. A number of ^{11}C-labeled D_2-agonists have been reported in recent years. Examples include [^{11}C](+)-PHNO (Ginovart et al., 2006, Narendran et al., 2006), [^{11}C]NPA (Hwang et al., 2000, Narendran et al., 2004), and [^{11}C]MNPA (Finnema et al., 2005, Seneca et al., 2006, Finnema et al., 2009). However, as with the radiolabeled antagonists described above, the binding potentials from PET studies with these radiotracers consist of a composite of the D_3 receptor and high affinity state of the D_2 receptor ($^{high}D_2$).

In previous efforts, our group structurally modified **NGB 2904** to yield the compounds **WC-10** and **LS-3-134**, which have high D_3 affinity, good D_3 vs. D_2 receptor selectivity, and favorable log P value to serve as radiotracers for *in vitro* and *in vivo* imaging studies of the D_3 receptor (Mach et al., 2011). **WC-10** has also been labeled with tritium, and [^{3}H]**WC-10** has proven to be a useful radioligand for *in vitro* autoradiography studies in rodent and nonhuman primate brain (Xu et al., 2009, Xu et al., 2010, Brown et al., 2011, Lim et al., 2011). We have also reported PET imaging studies of dopamine D_3 receptors using [^{18}F]**LS-3-134** (Mach et al., 2011), which can reproducibly image dopamine D_3 receptors in anesthetized nonhuman primates following the administration of the benzodiazepine agonist, lorazepam, to transiently reduce synaptic dopamine levels (Dewey et al., 1992, Nader et al., 2006).

In a similar manner, structural alteration of **Aripiprazole** (Abilify™), an atypical antipsychotic for treatment of schizophrenia, yielded the analog 7-(4-(4-(2-methoxyphenyl)piperazin-1-yl)butoxy)-3,4-dihydroquinolin-2(1H)-one oxalate (**SV-III-130**). **SV-III-130** has improved D_2 versus D_3 receptor selectivity in comparison with Aripirazole, a methoxy group for carbon-11 radiolabeling, and a favorable log P to serve as a radiotracer for PET imaging studies of the D_2 receptor (Vangveravong et al., 2011). In this study, we report the synthesis of [^{11}C]**SV-III-130**, a radiolabeled D_2 partial agonist that is capable of imaging the dopamine D_2 receptor *in vivo* with positron emission tomography. We also report evidence suggesting that there is a low level of competition between [^{11}C]**SV-III-130** and endogenous dopamine for D_2 receptors.

MATERIALS AND METHODS

Radiosynthesis

The synthesis of the *des*-methyl precursor, **SV-III-158**, and unlabeled **SV-III-130** (HPLC standard) was reported previously by our group (Vangveravong et al., 2011). [^{11}C]**SV-III-130** was prepared via O-alkylation of **SV-III-158** with [^{11}C]methyl iodide. The final product was purified by reversed-phase HPLC (C-18 column; 52% methanol: 48% ammonium formate buffer).

Receptor Binding Assays

In vitro binding assays for human dopamine receptors were conducted using the assay conditions described by Chu et al. in 2005. The radioligand used in the dopamine receptor binding assay was [^{125}I]IABN, which has a high affinity for dopamine D_2, D_3 and D_4 receptors (Luedtke et al., 2000). To measure the binding affinity at 5-HT$_{1A}$ receptors, a filtration binding assay previously described (Xu et al., 2005, Wang et al., 2011) was used with human 5-HT$_{1A}$ serotonin receptor membranes (ChanTest, Cleveland, OH, U.S.) and [^{3}H] 8-OH-DPAT (Perkin-Elmer, Boston, MA, U.S.) as the radioligand.

Intrinsic Activity Assay

The intrinsic activity at dopamine D_2 receptors was determined using the cAMP assay conditions as described in 2005 by Chu et al. (Chu et al., 2005). In this assay, quinpirole was used as a reference full agonist at both D_2 and D_3 dopamine receptors.

PET Data acquisition

MicroPET imaging studies were conducted on a Focus 220 microPET scanner (Siemens Medical Systems, Knoxville, TN, USA). Male rhesus monkeys (8 – 12 kg) were initially anesthetized with ketamine (10–15 mg/kg) and injected with glycopyrrolate (0.013 – 0.017 mg/kg) to reduce saliva secretions. PET tracers were administered ~ 90 minutes after ketamine injection. Subjects were intubated and placed on the scanner bed with a circulating warm water blanket and blankets. A water-soluble ophthalmic ointment was placed in the eyes, and the head was positioned in the center of the field using gauze rolls taped in place. Anesthesia was maintained with isoflurane (1.0 – 1.75 % in 1.5 L/min oxygen flow). Respiration rate, pulse, oxygen saturation, body temperature, and inspired/exhaled gasses were monitored throughout the study. Radiotracers and fluids were administered using a catheter placed percutaneously in a peripheral vein. For the metabolism studies, a catheter was placed percutaneously in the contralateral femoral artery to permit the collection of arterial blood samples and for the determination of the blood time-activity-curve using a continuous flow detection system (Hutchins et al., 1986). In each microPET scanning session, the head was positioned supine with the brain in the center of the field of view. A 10-minute transmission scan was performed to check positioning; once confirmed, a 45 minute transmission scan was obtained for attenuation correction. Subsequently, a 60-minute baseline dynamic emission scan was acquired after administration of ~10 mCi of [^{11}C]**SV-III-130** via the venous catheter. Displacement studies were also conducted in animals by administering compound *S*-(−)-eticlopride (0.025 mg/kg, i.v.), a nonselective dopamine D_2 and D_3 receptor ligand (Nader et al., 1999); and **WC-34**, a selective dopamine D_3 receptor ligand (Chu et al., 2005, Mach et al., 2011), 20 min post tracer injection. Chemical structures of *s*-(−)-eticlopride and **WC-34** and their binding affinities at dopamine receptors are shown in Figure 4. For the dopamine depletion studies, animals were given an intravenous dose of lorazepam (1 mg/kg in saline) approximately 30 min prior to injection of the radiotracer. For dopamine challenge studies, 1 mg/kg d-amphetamine was administrated via the venous catheter 20 min post radiotracer injection.

Time Activity Curves and Metabolite analysis

Arterial blood time activity curves for the initial 5 min post [^{11}C]**SV-III-130** injection were determined using the continuous flow detection system attached to a percutaneous arterial catheter. Arterial blood samples for metabolite analysis were taken in a heparinized syringe from the same catheter at 5 and 30 min post injection. The 5 min sample was taken immediately after the pump for the detector was turned off; the arterial line was flushed prior to collection of subsequent samples. Additional blood samples were taken at 10, 60 min for the TAC (Figure 5 C). Metabolite analysis was performed using a solid-phase extraction technique previously used for similar studies (Mach et al., 1997). A 1 mL aliquot of whole blood was centrifuged to separate plasma from packed red cells. Each fraction was counted, a 400 μL aliquot of plasma was removed, counted and deproteinated with 6 ml of 2: 1 methanol: 0.4 M perchloric acid mixture. After centrifugation the supernatant was diluted with 4 mL water and applied to an activated C-18 light Sep-Pak. The cartridge was neutralized with 2 mL 1N NaOH, then rinsed twice with water, and extracted with two portions of methanol (2 mL, 1 mL). All samples were counted in a Ludlum well counter. The methanol extracts were combined, concentrated in vacuo and rediluted to 150 μL of methanol for injection onto the HPLC. HPLC analysis was performed using a reversed-phase Phenomenex analytical column (Prodigy 250 × 4.6) with a mobile phase of methanol: 0.1 M ammonium formate buffer, pH 4.5 60:40. The flow rate was 0.8 ml/min, 0.5 min/ fraction; 36 fractions were collected and counted or each sample. The location of the parent UV peak was determined by injection of cold standard. After HPLC analysis of all plasma samples had been completed, the purity and stability of the injectate were confirmed by analysis of both reserved injectate and an *in vitro* control (reserved injectate added to a pre-scan blood sample which was immediately processed as described above). This control also confirmed the stability of the radiotracer under the conditions used to process the blood for metabolite analysis. The percentages of unchanged parent compound and its metabolites were determined by decay correcting the counts and dividing the amount of recovered activity in all samples and multiplying by 100. (Table 2) Only a single peak for the parent compound was observed in the *in vitro* control and > 95% of the activity was recovered.

Image processing and analysis

Acquired list mode data were histogrammed into a 3D set of sinograms and binned to the following time frames: 3×1 min, 4×2 min, 3×3 min and 20×5 min. Sinogram data were corrected for attenuation and scatter. Maximum a posteriori (MAP) reconstructions were done with 18 iterations and a beta value of 0.004, resulting in a final $256 \times 256 \times 95$ matrix. The voxel dimensions of the reconstructed images were $0.95 \times 0.95 \times 0.80$ mm^3. A 1.5 mm Gaussian filter was applied to smooth each MAP reconstructed image. These images were then co-registered with MRI images to identify the regions of interest with AnalyzeDirect software (AnalyzeDirect, Inc., Overland Park, KS). 3D regions of interest PET images were manually drawn using co-registered MRI images as references for the caudate, putamen and cerebellum to obtain time–activity curves. Activity measures were standardized to dose of radioactivity injected to yield %ID/c.c. (Figure 5 A and B.). Logan DVR-1 (binding potential) analyses were performed using the cerebellum as the reference region, with a K_2 value of 0.035 (Logan, 2000). Percent dopamine (DA) occupancy (OCC) in the caudate and putamen was measured as $(1-[DVR_{baseline} -1]/[DVR_{d\text{-}amphetamine} -1]) \times 100$ (Mukherjee et al., 2001).

RESULTS

In vitro binding studies indicate that **SV-III-130** (Figure 1) has a high affinity for D_2 receptors (0.22 nM) and ~60-fold selectivity for D_2 versus D_3 receptors (Table 1). Functional assays demonstrated that **SV-III-130** partially inhibited forskolin-dependent

adenylyl cyclase activity relative to quinpirole (~ 61% maximal response) in CHO cells transfected with $^hD_2$ receptors (Table 1), indicating that it is a partial agonist at D_2 receptors. The affinity of **SV-III-130** for dopamine D_4 receptors was low (~210 nM). It's noteworthy that **SV-III-130** also has high binding affinity for 5-HT$_{1A}$ receptor (0.28 nM).

The synthesis of [^{11}C]**SV-III-130** was achieved in approximately 60 min in an overall radiochemical yield of 60% from starting [^{11}C]methyl iodide. The specific activity of the final compound was ~3,000 mCi/μmol (end of bombardment); radiochemical purity was greater than 95% and suitable for microPET imaging studies (Figure 2).

Metabolism studies of arterial blood samples indicated that [^{11}C]**SV-III-130** is relatively stable; the 30 minute blood sample post-i.v. administration of the radiotracer contained greater than 60% parent compound (Table 2).

MicroPET studies were conducted in rhesus monkeys under 1% isoflurane anesthesia (n = 4). These initial baseline microPET imaging studies (Figure 3, top panel) demonstrated high uptake of [^{11}C]**SV-III-130** in the caudate and putamen. A second series of studies were conducted in which the animal received an intravenous dose of lorazepam (1.0 mg/kg) 30 min prior to the injection of the radiotracer (Figure 3, bottom panel). Lorazepam has been shown to increase striatal [^{11}C]raclopride binding (Dewey et al., 1992); we previously used this paradigm to evaluate the effect of endogenous dopamine on the binding of the dopamine $D_{2/3}$ radiotracer, [^{18}F]FCP, and the dopamine D_3 radiotracer [^{18}F]**LS-3-134** in rhesus monkeys (Nader et al., 2006, Mach et al., 2011). The tissue-time activity curves in the lorazepam-treated animals were similar to the baseline study (Figure 5 A and B). Pretreatment with lorazepam had no significant effects on the binding of [^{11}C]**SV-III-130** to dopamine D_2 receptors as measured by the Logan DVR-1 analyses (Figure 6) (Logan, 2000). There was no obvious binding of [^{11}C]**SV-III-130** in the thalamus, a region known to express D_3 versus D_2 receptors (Rabiner et al., 2009, Sun et al., 2012) under either baseline and lorazemap depletion conditions. This data indicate that [^{11}C]**SV-III-130** does not label dopamine D_3 receptors *in vivo*. In contrast to the depletion of endogenous dopamine with lorazepam, dopamine challenge studies resulting from the administration of d-amphetamine (1 mg/kg/i.v.) 20 minutes post-i.v. injection of the radiotracer resulted in a displacement of [^{11}C]**SV-III-130** in the caudate and putamen (Figure 5 C). Binding potential analyses demonstrated that the effect of d-amphetamine is significant for both caudate (p = 0.0001) and putamen (p = 0.03) (Table 3). Percent dopamine (DA) occupancy (OCC) is higher in the caudate than in the putamen for all 4 monkeys. Rapid displacement in the caudate and putamen, but not in the cerebellum, was observed after injection of the dopamine $D_{2/3}$ nonselective ligand S(–)-eticlopride at a relatively low dosage (0.025 mg/kg/i.v.) (Figure 5 D). These data indicate that the binding of [^{11}C]**SV-III-130** to D_2 receptors in the caudate and putamen is reversible. A dopamine D_3 receptor selective ligand **WC-34** (0.025 mg/kg/i.v.) didn't displace the binding of [^{11}C]**SV-III-130** in the caudate and putamen, which suggests that the binding of [^{11}C]**SV-III-130** is specific to dopamine D_2 v.s. D_3 receptors. [^{11}C]**SV-III-130** activity uptake in the blood peaked at ~ 1 minute post tracer injection and displayed rapid blood activity clearance (Figure 5 F and G).

DISCUSSION

Despite the structure similarities and high degree of sequence homology in the ligand binding domains (Sokoloff et al., 1990), the D_2 and D_3 receptors are thought to differ in their a) neuroanatomical localization, b) levels of receptor expression, c) efficacy in response to agonist stimulation, and d) regulation and desensitization (Joyce, 2001, Luedtke and Mach, 2003, Mach et al., 2004). However, the absolute densities of D_2 and D_3 receptors, and the differential expression of these receptors in the CNS, is currently not known since

there are no selective radioligands to measure D_2 versus D_3 receptors, and vice versa, using either *in vitro* (autoradiography) or *in vivo* (PET) imaging techniques. Although a number of dopamine D_2 and D_3 selective radiotracers, labeled with either carbon-11 (t = 20.4 min) or fluorine-18 (t = 110 min), have been reported over the past twenty years, none have proven to be useful for selectively imaging dopamine D_2 or D_3 receptors *in vivo*. Nonselective dopamine D_2/D_3 radiotracers inevitably provide a binding potential from the combination of both receptor signals, such as the radiolabeled antagonists [11C]raclopride (Yokoi et al., 2002, Volkow et al., 2008), [11C]fallypride or [18F]fallypride (Buchsbaum et al., 2006, Narendran et al., 2009); and [11C]FLB457 (Cselenyi et al., 2006, Vandehey et al., 2010), and full agonists at D_2 and D_3 receptors, [11C](+)-PHNO (Ginovart et al., 2006, Narendran et al., 2006), [11C]NPA (Hwang et al., 2000, Narendran et al., 2004), and [11C]MNPA (Finnema et al., 2005, Seneca et al., 2006, Finnema et al., 2009).

In a previous study, we reported that [18F]**LS-3-134** has a subnanomolar affinity for dopamine D_3 receptors and a 160-fold higher affinity for D_3 compared to D_2 dopamine receptors (Mach et al., 2011). Because of the high affinity of dopamine for D_3 receptors, it was necessary to deplete the synapse dopamine of [18F]**LS-3-134** in anesthetized rhesus monkeys in order to image the D_3 receptor. These data are consistent with previous reports demonstrating that there is a high *in vivo* occupancy of D_3 receptors by endogenous dopamine (Schotte et al., 1992, Schotte et al., 1996). That study also demonstrated that [18F]**LS-3-134** had high binding in the thalamus which is believed to be a brain region having a high density of D_3 receptors (Rabiner et al., 2009, Sun et al., 2012). In the current study, we found [11C]**SV-III-130** had high binding in the caudate and putamen and no uptake in the thalamus. Dopamine depletion did not increase the uptake of the radiotracer in the caudate, putamen and thalamus. These data suggest [11C]**SV-III-130** binding to dopamine D_3 receptors is negligible since there was no tracer uptake in the thalamus under both baseline and dopamine depletion conditions. Recently it was reported that dopamine D_2 receptor preferring ligand [18F](*N*-Methyl)Benperidol (NMB) has appreciable binding in the thalamus (Eisenstein et al., 2012); this very likely represents binding at dopamine D_4 receptors since [18F]NMB has a high binding affinity at the D_4 receptor (K_i = 4.9 nM), and there is a high density of D_4 receptors in the thalamus (Primus et al., 1997, Karimi et al., 2011). The observation that dopamine depletion did not change the binding potential of [11C]**SV-III-130** in the caudate and putamen also suggests that endogenous dopamine has a low *in vivo* occupancy at D_2 receptors. This result agrees well with previous reports that endogenous dopamine protects the D_3 receptor (but not the D_2) receptors from alkylation by 1-ethoxycarbonyl-2-ethoxy-1,2-dihydroquinoline (EEDQ) and the spiperone analog, N-(*p*-isothiocyanatophenethyl)spiperone (NIPS) (Levant, 1995, Zhang et al., 1999). Occupancy of D_3 receptors by endogenous dopamine *in vivo* is high due to the higher binding affinity of dopamine for dopamine D_3 versus D_2 receptors (Levant, 1997).

Unlike the dopamine depletion studies using lorazepam, d-amphetamine challenge given 20 min post-i.v. injection of the radiotracer resulted in a change (i.e., reduction) of [11C]**SV-III-130** binding in the caudate and putamen. This reduction in tracer binding is believed to be caused by the *in vivo* displacement of radiotracer by d-amphetamine-induced elevations in synaptic dopamine levels. A higher percent dopamine (DA) occupancy (OCC) was observed in the caudate than in the putamen, which is consistent with a previous report using [18F]fallypride as the radioligand (Mukherjee et al., 2005). To confirm the displaceable binding of [11C]**SV-III-130** to dopamine D_2 receptors in the caudate and putamen, a low dose of the $D_{2/3}$ antagonist *S*(−)-eticlopride (0.025 mg/kg/i.v.) was administered at 20 min post-i.v. injection of the radiotracer. S(−)-eticlopride rapidly displaced [11C]**SV-III-130** binding in the caudate and putamen, with the striatal activity reached a level close to that in the reference region of cerebellum by ~ 50 min post-injection. To test the specificity of [11C]**SV-III-130** binding to dopamine D_2 but not D_3 receptors, a relatively high dose (4 fold

higher of that of $s(-)$-eticlopride, i.e., 0.1 mg/kg/i.v.) of selective D_3 receptor partial agonist **WC-34** was administered at 20 min post-i.v. injection of the radiotracer, no obvious displacement of [^{11}C]**SV-III-130** was observed.

Although the *in vitro* binding assay showed that **SV-III-130** has a high binding affinity for 5-HT$_{1A}$ receptor, the *in vivo* PET imaging studies didn't suggest that [^{11}C]**SV-III-130** labeled 5-HT$_{1A}$ sites in the nonhuman primate brains; no obvious uptake was detected in the 5-HT$_{1A}$ receptor enriched regions, such as the dorsal raphe, cingulate cortex and hippocampus(Saigal et al., 2006).

In summary, we have evaluated the *in vivo* properties of [^{11}C]**SV-III-130**, a radiotracer with subnanomolar affinity for dopamine D_2 receptors and 60-fold selectivity over dopamine D_3 receptors. Preclinical imaging studies using nonhuman primates indicates [^{11}C]**SV-III-130** images dopamine D_2 but not D_3 receptors. This study also demonstrated that dopamine D_2 receptors can be imaged in nonhuman primates without the need to deplete the dopaminergic synapses of endogenous neurotransmitter, which is in stark contrast to the imaging of D_3 receptors with the radiotracer [^{18}F]**LS-3134**. Translational imaging studies in human subjects are clearly needed to determine the ability of [^{11}C]**SV-III-130** to directly measure dopamine D_2 receptors without interference from the labeling of D_3 receptors.

Acknowledgments

References

Brown JA, Xu J, Diggs-Andrews KA, Wozniak DF, Mach RH, Gutmann DH. PET imaging for attention deficit preclinical drug testing in neurofibromatosis-1 mice. Experimental neurology. 2011; 232:333–338. [PubMed: 21963652]

Buchsbaum MS, Christian BT, Lehrer DS, Narayanan TK, Shi B, Mantil J, Kemether E, Oakes TR, Mukherjee J. D2/D3 dopamine receptor binding with [F-18]fallypride in thalamus and cortex of patients with schizophrenia. Schizophr Res. 2006; 85:232–244. [PubMed: 16713185]

Chu W, Tu Z, McElveen E, Xu J, Taylor M, Luedtke RR, Mach RH. Synthesis and in vitro binding of N-phenyl piperazine analogs as potential dopamine D3 receptor ligands. Bioorg Med Chem. 2005; 13:77–87. [PubMed: 15582454]

Cselenyi Z, Olsson H, Halldin C, Gulyas B, Farde L. A comparison of recent parametric neuroreceptor mapping approaches based on measurements with the high affinity PET radioligands [11C]FLB 457 and [11C]WAY 100635. Neuroimage. 2006; 32:1690–1708. [PubMed: 16859930]

Dewey SL, Smith GS, Logan J, Brodie JD, Yu DW, Ferrieri RA, King PT, MacGregor RR, Martin TP, Wolf AP, et al. GABAergic inhibition of endogenous dopamine release measured in vivo with 11C-raclopride and positron emission tomography. J Neurosci. 1992; 12:3773–3780. [PubMed: 1357114]

Eisenstein SA, Koller JM, Piccirillo M, Kim A, Antenor-Dorsey JA, Videen TO, Snyder AZ, Karimi M, Moerlein SM, Black KJ, Perlmutter JS, Hershey T. Characterization of extrastriatal D2 in vivo specific binding of [18F](N-methyl)benperidol using PET. Synapse. 2012; 66:770–780. [PubMed: 22535514]

Finnema SJ, Halldin C, Bang-Andersen B, Gulyas B, Bundgaard C, Wikstrom HV, Farde L. Dopamine D(2/3) receptor occupancy of apomorphine in the nonhuman primate brain--a comparative PET study with [11C]raclopride and [11C]MNPA. Synapse. 2009; 63:378–389. [PubMed: 19173265]

Finnema SJ, Seneca N, Farde L, Shchukin E, Sovago J, Gulyas B, Wikstrom HV, Innis RB, Neumeyer JL, Halldin C. A preliminary PET evaluation of the new dopamine D2 receptor agonist [11C]MNPA in cynomolgus monkey. Nucl Med Biol. 2005; 32:353–360. [PubMed: 15878504]

Ginovart N, Galineau L, Willeit M, Mizrahi R, Bloomfield PM, Seeman P, Houle S, Kapur S, Wilson AA. Binding characteristics and sensitivity to endogenous dopamine of [11C]-(+)-PHNO, a new agonist radiotracer for imaging the high-affinity state of D2 receptors in vivo using positron emission tomography. J Neurochem. 2006; 97:1089–1103. [PubMed: 16606355]

Herve D, Le Moine C, Corvol JC, Belluscio L, Ledent C, Fienberg AA, Jaber M, Studler JM, Girault JA. Galpha(olf) levels are regulated by receptor usage and control dopamine and adenosine action in the striatum. J Neurosci. 2001; 21:4390–4399. [PubMed: 11404425]

Hutchins GD, Hichwa RD, Koeppe RA. A Continuous Flow Input Function Detector for H2 15O Blood Flow Studies in Positron Emission Tomography. Nuclear Science, IEEE Transactions on. 1986; 33:546–549.

Hwang DR, Kegeles LS, Laruelle M. (−)-N-[(11C]propyl-norapomorphine: a positron-labeled dopamine agonist for PET imaging of D(2) receptors. Nucl Med Biol. 2000; 27:533–539. [PubMed: 11056366]

Jardemark K, Wadenberg ML, Grillner P, Svensson TH. Dopamine D3 and D4 receptor antagonists in the treatment of schizophrenia. Curr Opin Investig Drugs. 2002; 3:101–105.

Joyce JN. Dopamine D3 receptor as a therapeutic target for antipsychotic and antiparkinsonian drugs. Pharmacol Ther. 2001; 90:231–259. [PubMed: 11578658]

Kapur S, Mamo D. Half a century of antipsychotics and still a central role for dopamine D2 receptors. Prog Neuropsychopharmacol Biol Psychiatry. 2003; 27:1081–1090. [PubMed: 14642968]

Karimi M, Moerlein SM, Videen TO, Luedtke RR, Taylor M, Mach RH, Perlmutter JS. Decreased striatal dopamine receptor binding in primary focal dystonia: a D2 or D3 defect? Movement disorders: official journal of the Movement Disorder Society. 2011; 26:100–106. [PubMed: 20960437]

Korczyn AD. Dopaminergic drugs in development for Parkinson's disease. Adv Neurol. 2003; 91:267–271. [PubMed: 12442685]

Lee T, Seeman P, Rajput A, Farley IJ, Hornykiewicz O. Receptor basis for dopaminergic supersensitivity in Parkinson's disease. Nature. 1978; 273:59–61. [PubMed: 692671]

Levant B. Differential sensitivity of [3H]7-OH-DPAT-labeled binding sites in rat brain to inactivation by N-ethoxycarbonyl-2-ethoxy-1,2-dihydroquinoline. Brain Res. 1995; 698:146–154. [PubMed: 8581473]

Levant B. The D3 dopamine receptor: neurobiology and potential clinical relevance. Pharmacological reviews. 1997; 49:231–252. [PubMed: 9311022]

Lim MM, Xu J, Holtzman DM, Mach RH. Sleep deprivation differentially affects dopamine receptor subtypes in mouse striatum. Neuroreport. 2011; 22:489–493. [PubMed: 21642879]

Logan J. Graphical analysis of PET data applied to reversible and irreversible tracers. Nucl Med Biol. 2000; 27:661–670. [PubMed: 11091109]

Luedtke RR, Freeman RA, Boundy VA, Martin MW, Huang Y, Mach RH. Characterization of (125)I-IABN, a novel azabicyclononane benzamide selective for D2-like dopamine receptors. Synapse. 2000; 38:438–449. [PubMed: 11044891]

Luedtke RR, Mach RH. Progress in developing D3 dopamine receptor ligands as potential therapeutic agents for neurological and neuropsychiatric disorders. Curr Pharm Des. 2003; 9:643–671. [PubMed: 12570797]

Mach RH, Huang Y, Freeman RA, Wu L, Vangveravong S, Luedtke RR. Conformationally-flexible benzamide analogues as dopamine D3 and sigma 2 receptor ligands. Bioorg Med Chem Lett. 2004; 14:195–202. [PubMed: 14684327]

Mach RH, Nader MA, Ehrenkaufer RL, Line SW, Smith CR, Gage HD, Morton TE. Use of positron emission tomography to study the dynamics of psychostimulant-induced dopamine release. Pharmacol Biochem Behav. 1997; 57:477–486. [PubMed: 9218272]

Mach RH, Tu Z, Xu J, Li S, Jones LA, Taylor M, Luedtke RR, Derdeyn CP, Perlmutter JS, Mintun MA. Endogenous dopamine (DA) competes with the binding of a radiolabeled D(3) receptor partial agonist in vivo: a positron emission tomography study. Synapse. 2011; 65:724–732. [PubMed: 21132811]

Missale C, Nash SR, Robinson SW, Jaber M, Caron MG. Dopamine receptors: from structure to function. Physiol Rev. 1998; 78:189–225. [PubMed: 9457173]

Mukherjee J, Christian BT, Narayanan TK, Shi B, Collins D. Measurement of d-amphetamine-induced effects on the binding of dopamine D-2/D-3 receptor radioligand, 18F-fallypride in extrastriatal brain regions in non-human primates using PET. Brain Res. 2005; 1032:77–84. [PubMed: 15680944]

Mukherjee J, Christian BT, Narayanan TK, Shi B, Mantil J. Evaluation of dopamine D-2 receptor occupancy by clozapine, risperidone, and haloperidol in vivo in the rodent and nonhuman primate brain using 18F-fallypride. Neuropsychopharmacology. 2001; 25:476–488. [PubMed: 11557161]

Nader MA, Green KL, Luedtke RR, Mach RH. The effects of benzamide analogues on cocaine self-administration in rhesus monkeys. Psychopharmacology (Berl). 1999; 147:143–152. [PubMed: 10591881]

Nader MA, Morgan D, Gage HD, Nader SH, Calhoun TL, Buchheimer N, Ehrenkaufer R, Mach RH. PET imaging of dopamine D2 receptors during chronic cocaine self-administration in monkeys. Nat Neurosci. 2006; 9:1050–1056. [PubMed: 16829955]

Narendran R, Frankle WG, Mason NS, Rabiner EA, Gunn RN, Searle GE, Vora S, Litschge M, Kendro S, Cooper TB, Mathis CA, Laruelle M. Positron emission tomography imaging of amphetamine-induced dopamine release in the human cortex: a comparative evaluation of the high affinity dopamine D2/3 radiotracers [11C]FLB 457 and [11C]fallypride. Synapse. 2009; 63:447–461. [PubMed: 19217025]

Narendran R, Hwang DR, Slifstein M, Talbot PS, Erritzoe D, Huang Y, Cooper TB, Martinez D, Kegeles LS, Abi-Dargham A, Laruelle M. In vivo vulnerability to competition by endogenous dopamine: comparison of the D2 receptor agonist radiotracer (−)-N-[11C]propyl-norapomorphine ([11C]NPA) with the D2 receptor antagonist radiotracer [11C]-raclopride. Synapse. 2004; 52:188–208. [PubMed: 15065219]

Narendran R, Slifstein M, Guillin O, Hwang Y, Hwang DR, Scher E, Reeder S, Rabiner E, Laruelle M. Dopamine (D2/3) receptor agonist positron emission tomography radiotracer [11C]-(+)-PHNO is a D3 receptor preferring agonist in vivo. Synapse. 2006; 60:485–495. [PubMed: 16952157]

Nieoullon A. Dopamine and the regulation of cognition and attention. Prog Neurobiol. 2002; 67:53–83. [PubMed: 12126656]

Primus RJ, Thurkauf A, Xu J, Yevich E, McInerney S, Shaw K, Tallman JF, Gallagher DW. II. Localization and characterization of dopamine D4 binding sites in rat and human brain by use of the novel, D4 receptor-selective ligand [3H]NGD 94-1. The Journal of pharmacology and experimental therapeutics. 1997; 282:1020–1027. [PubMed: 9262371]

Rabiner EA, Slifstein M, Nobrega J, Plisson C, Huiban M, Raymond R, Diwan M, Wilson AA, McCormick P, Gentile G, Gunn RN, Laruelle MA. In vivo quantification of regional dopamine-D3 receptor binding potential of (+)-PHNO: Studies in non-human primates and transgenic mice. Synapse. 2009; 63:782–793. [PubMed: 19489048]

Saigal N, Pichika R, Easwaramoorthy B, Collins D, Christian BT, Shi B, Narayanan TK, Potkin SG, Mukherjee J. Synthesis and biologic evaluation of a novel serotonin 5-HT1A receptor radioligand, 18F-labeled mefway, in rodents and imaging by PET in a nonhuman primate. Journal of nuclear medicine: official publication, Society of Nuclear Medicine. 2006; 47:1697–1706.

Schotte A, Janssen P, Bonaventure P, Leysen J. Endogenous dopamine limits the binding of antipsychotic drugs to D3 receptors in the rat brain: a quantitative autoradiographic study. The Histochemical Journal. 1996; 28:791–799. [PubMed: 8968731]

Schotte A, Janssen PF, Gommeren W, Luyten WH, Leysen JE. Autoradiographic evidence for the occlusion of rat brain dopamine D3 receptors in vivo. Eur J Pharmacol. 1992; 218:373–375. [PubMed: 1425949]

Sealfon SC, Olanow CW. Dopamine receptors: from structure to behavior. Trends Neurosci. 2000; 23:S34–40. [PubMed: 11052218]

Seneca N, Finnema SJ, Farde L, Gulyas B, Wikstrom HV, Halldin C, Innis RB. Effect of amphetamine on dopamine D2 receptor binding in nonhuman primate brain: a comparison of the agonist radioligand [11C]MNPA and antagonist [11C]raclopride. Synapse. 2006; 59:260–269. [PubMed: 16416444]

Sibley DR, Monsma FJ Jr. Molecular biology of dopamine receptors. Trends Pharmacol Sci. 1992; 13:61–69. [PubMed: 1561715]

Sokoloff P, Giros B, Martres MP, Bouthenet ML, Schwartz JC. Molecular cloning and characterization of a novel dopamine receptor (D3) as a target for neuroleptics. Nature. 1990; 347:146–151. [PubMed: 1975644]

Sun J, Xu J, Cairns NJ, Perlmutter JS, Mach RH. Dopamine D(1), D(2), D(3) Receptors, Vesicular Monoamine Transporter Type-2 (VMAT2) and Dopamine Transporter (DAT) Densities in Aged Human Brain. PloS one. 2012; 7:e49483. [PubMed: 23185343]

Uhl GR, Vandenbergh DJ, Rodriguez LA, Miner L, Takahashi N. Dopaminergic genes and substance abuse. Adv Pharmacol. 1998; 42:1024–1032. [PubMed: 9328073]

Vallone D, Picetti R, Borrelli E. Structure and function of dopamine receptors. Neurosci Biobehav Rev. 2000; 24:125–132. [PubMed: 10654668]

Vandehey NT, Moirano JM, Converse AK, Holden JE, Mukherjee J, Murali D, Nickles RJ, Davidson RJ, Schneider ML, Christian BT. High-affinity dopamine D2/D3 PET radioligands 18F-fallypride and 11C-FLB457: a comparison of kinetics in extrastriatal regions using a multiple-injection protocol. J Cereb Blood Flow Metab. 2010; 30:994–1007. [PubMed: 20040928]

Vangveravong S, Zhang Z, Taylor M, Bearden M, Xu J, Cui J, Wang W, Luedtke RR, Mach RH. Synthesis and characterization of selective dopamine D(2) receptor ligands using aripiprazole as the lead compound. Bioorg Med Chem. 2011; 19:3502–3511. [PubMed: 21536445]

Volkow ND, Fowler JS, Wang GJ. Role of dopamine in drug reinforcement and addiction in humans: results from imaging studies. Behav Pharmacol. 2002; 13:355–366. [PubMed: 12394411]

Volkow ND, Wang GJ, Telang F, Fowler JS, Logan J, Wong C, Ma J, Pradhan K, Tomasi D, Thanos PK, Ferre S, Jayne M. Sleep deprivation decreases binding of [11C]raclopride to dopamine D2/D3 receptors in the human brain. J Neurosci. 2008; 28:8454–8461. [PubMed: 18716203]

Wang W, Cui J, Lu X, Padakanti PK, Xu J, Parsons SM, Luedtke RR, Rath NP, Tu Z. Synthesis and in vitro biological evaluation of carbonyl group-containing analogues for sigma1 receptors. J Med Chem. 2011; 54:5362–5372. [PubMed: 21732626]

Xu J, Chu W, Tu Z, Jones LA, Luedtke RR, Perlmutter JS, Mintun MA, Mach RH. [(3)H]4-(Dimethylamino)-N-[4-(4-(2-methoxyphenyl)piperazin- 1-yl)butyl]benzamide, a selective radioligand for dopamine D(3) receptors. I. In vitro characterization. Synapse. 2009; 63:717–728. [PubMed: 19425052]

Xu J, Hassanzadeh B, Chu W, Tu Z, Jones LA, Luedtke RR, Perlmutter JS, Mintun MA, Mach RH. [3H]4-(dimethylamino)-N-(4-(4-(2-methoxyphenyl)piperazin-1-yl) butyl)benzamide: a selective radioligand for dopamine D3 receptors. II. Quantitative analysis of dopamine D3 and D2 receptor density ratio in the caudate-putamen. Synapse. 2010; 64:449–459. [PubMed: 20175227]

Xu J, Tu Z, Jones LA, Vangveravong S, Wheeler KT, Mach RH. [3H]N-[4-(3,4-dihydro-6,7-dimethoxyisoquinolin-2(1H)-yl)butyl]-2-methoxy-5-methyl benzamide: a novel sigma-2 receptor probe. Eur J Pharmacol. 2005; 525:8–17. [PubMed: 16289030]

Yokoi F, Grunder G, Biziere K, Stephane M, Dogan AS, Dannals RF, Ravert H, Suri A, Bramer S, Wong DF. Dopamine D2 and D3 receptor occupancy in normal humans treated with the antipsychotic drug aripiprazole (OPC 14597): a study using positron emission tomography and [11C]raclopride. Neuropsychopharmacology. 2002; 27:248–259. [PubMed: 12093598]

Zhang K, Weiss NT, Tarazi FI, Kula NS, Baldessarini RJ. Effects of alkylating agents on dopamine D3 receptors in rat brain: selective protection by dopamine. Brain Res. 1999; 847:32–37. [PubMed: 10564733]

Highlights

- We synthesized a novel dopamine D_2 receptor radiotracer, $[^{11}C]$**SV-III-130**.

- We conducted microPET imaging of dopamine D_2 receptors using $[^{11}C]$**SV-III-130**.

- $[^{11}C]$**SV-III-130** binding can be displaced $D_{2/3}$ ligand $S(-)$-eticlopride.

- Dopamine depletion via lorazepam treatment didn't change the binding potential.

- D-amphetamine induced dopamine increase displaced $[^{11}C]$**SV-III-130** binding.

$[^{11}C]$SV-III-130

$^hD_2 = 0.22$ nM

$^hD_3 = 13.1$ nM

$^hD_4 = 212$ nM

5-HT$_{1A}$ = 0.28 nM

Log P = 3.67
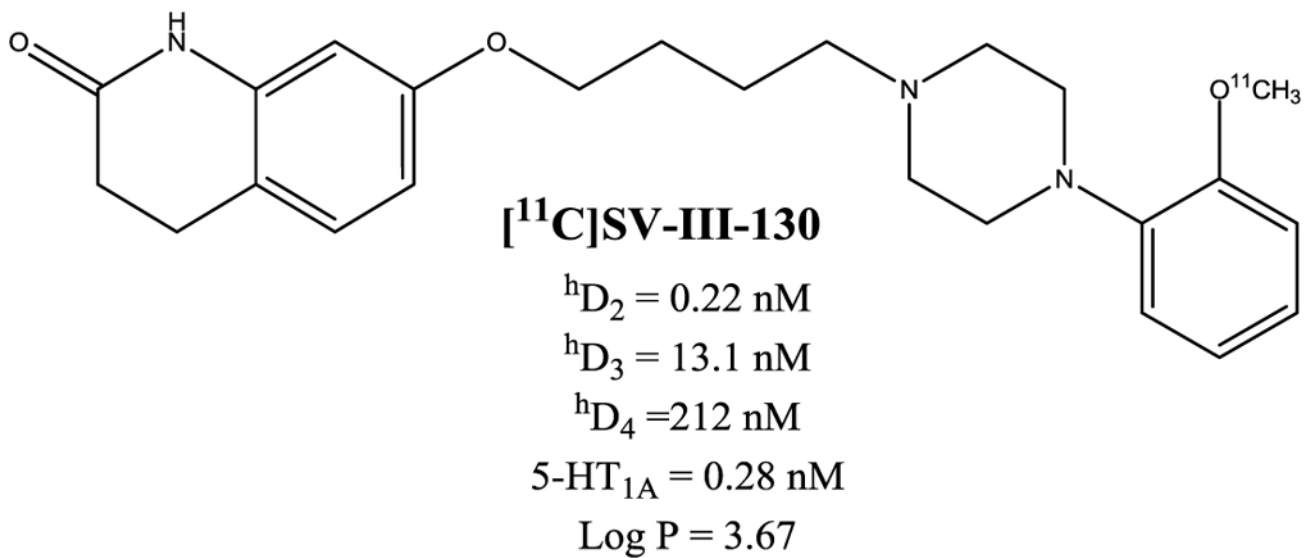
Figure 1.
Structure and pharmacology of D$_2$-selective ligand **SV-III-130**. A summary of **SV-III-130**'s binding affinity (dissociation constants) for human dopamine D$_2$, D$_3$, D$_4$ and serotonin 5-HT$_{1A}$ receptors are shown. The theoretical values for the partition coefficient, log P, was obtained using ChemDraw. Pharmacological data for dopamine receptors are taken from Vangveravong et al., 2011.
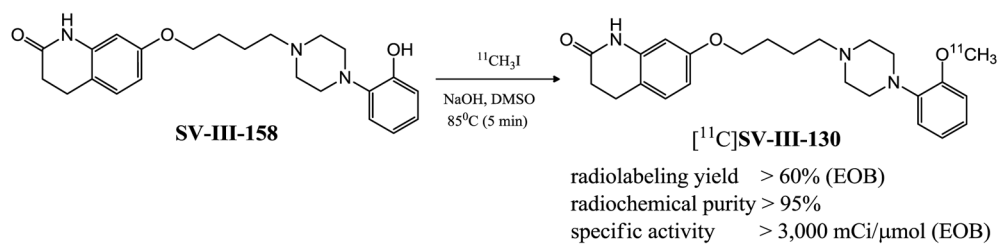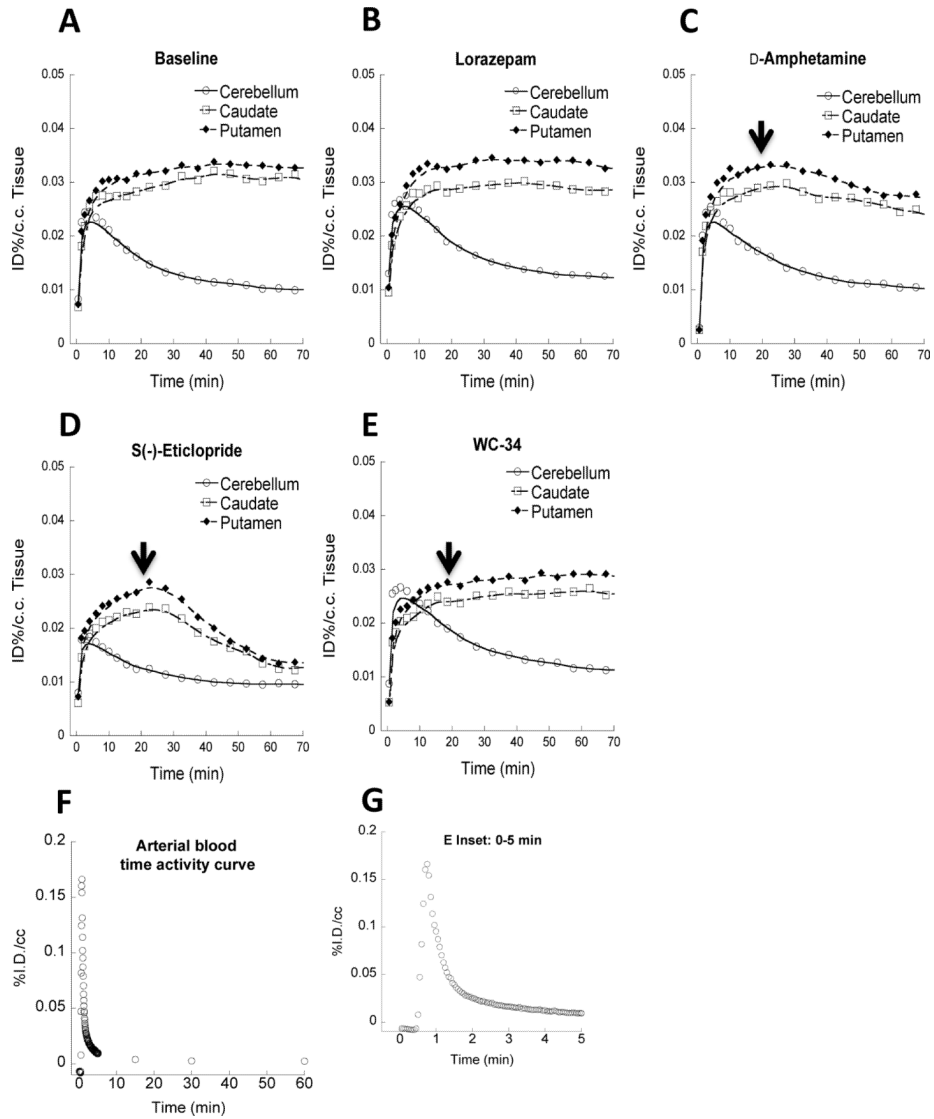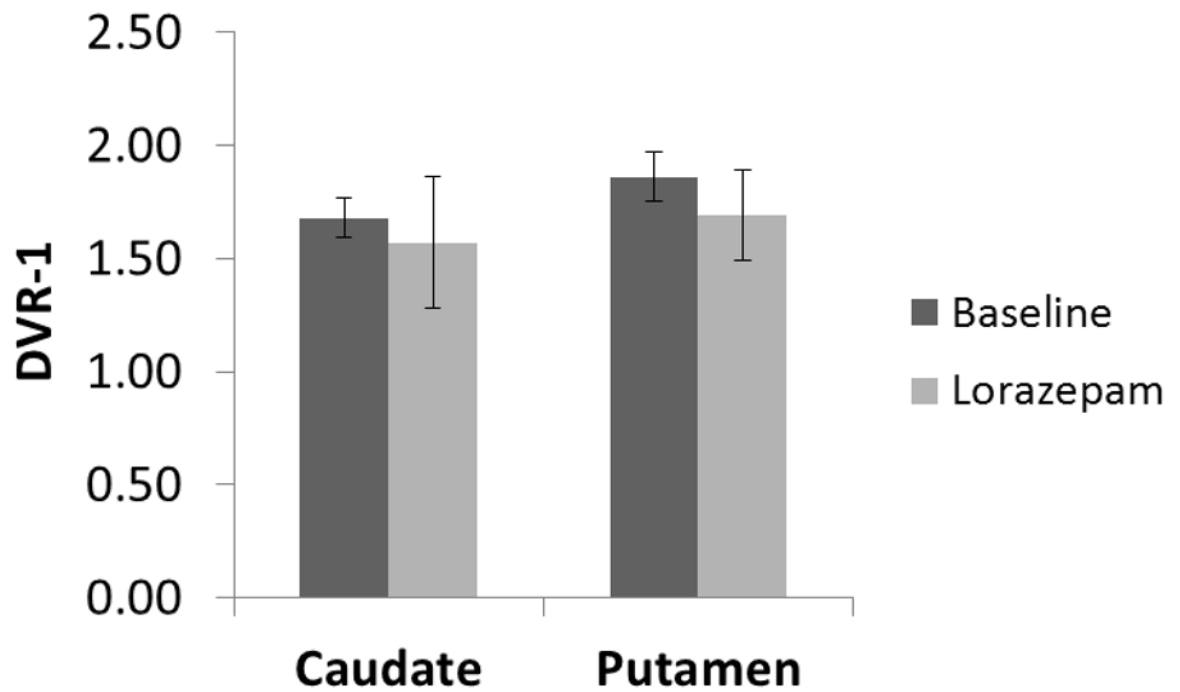
Figure 2.
Radiosynthesis of [^{11}C]**SV-III-130**.
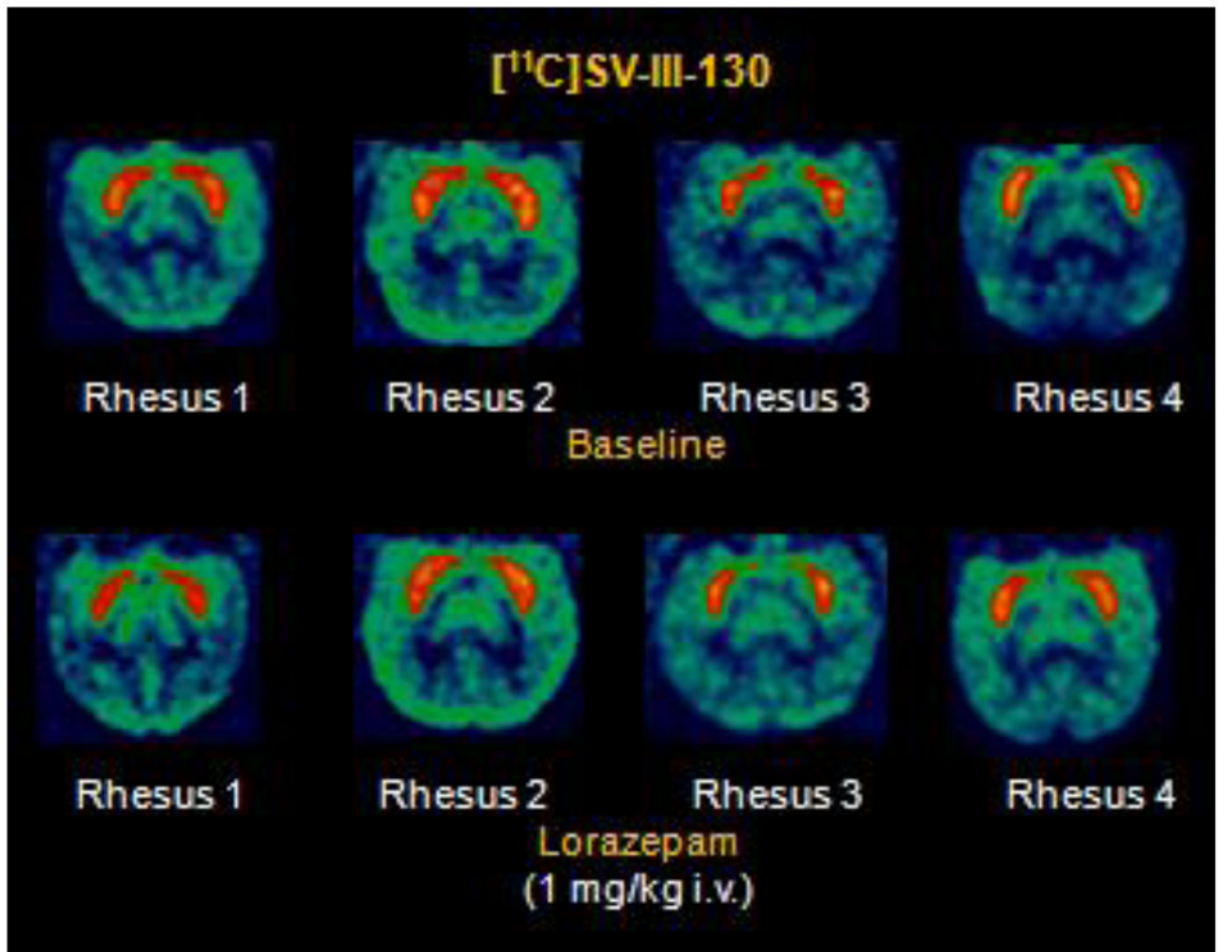
Figure 3.
MicroPET imaging studies of [11C]**SV-III-130** in rhesus monkeys.
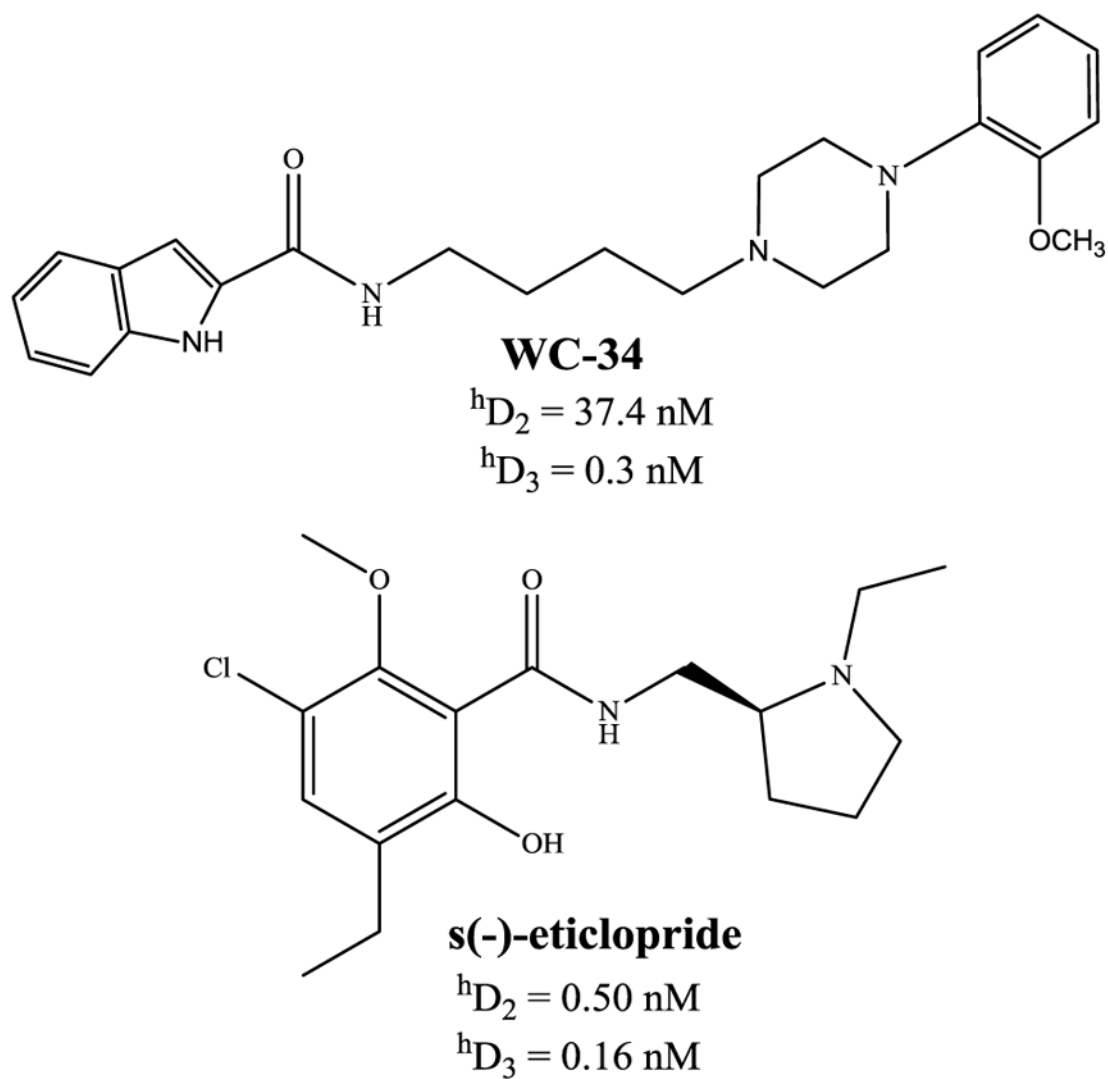
Figure 4.
Structures and pharmacology of a nonselective dopamine $D_{2/3}$ receptor ligand s(−)-eticlopride and a selective dopamine D_3 receptor ligand **WC-34**. A summary of binding affinities (dissociation constants) for human dopamine D_2 and D_3 receptors are shown. Pharmacological data are taken from Chu et al., 2005 and Nader et al., 1999.

Figure 5.
Representative blood and Tissue time-activity curves (TACs) of [^{11}C]**SV-III-130** from microPET imaging studies. **A** and **B** show regional brain TACs from baseline and lorazepam studies. The uptake of [^{11}C]**SV-III-130** in the representative monkey brain regions (caudate, putamen and cerebellum) reached peak accumulation in the caudate and putamen 10 min post-i.v. injection. Lorazepam (1 mg/kg/i.v.) treatment didn't increase [^{11}C]**SV-III-130** uptake in the caudate and putamen. **C** shows that 1 mg/kg d-amphetamine challenge slightly decreased [^{11}C]**SV-III-130** uptake in the caudate and putamen. Arrow shows the time point (20 min) when d-amphetamine was administrated. **D** shows that [^{11}C]**SV-III-130** uptake in the caudate and putamen was reversible, 0.025 mg/kg/i.v. s(−)-eticlopride rapidly displaced [^{11}C]**SV-III-130** binding to dopamine D$_2$ receptors in the caudate and putamen. **E** shows that [^{11}C]**SV-III-130** uptake in the caudate and putamen was specific to dopamine D$_2$ receptors, which was not displaced by 0.1 mg/kg/i.v. **WC-34**, a dopamine D$_3$ receptor selective ligand. **F** shows the arterial blood TAC. The inset graph **G** shows the TAC of the initial 5 minutes.

Figure 6.
Binding potential (DVR-1) analysis in caudate and putamen of microPET scans from baseline (test-retest average), lorazepam treatment and d-amphetamine challenge studies. Lorazepam has no significant effects on the [^{11}C]**SV-III-130** binding potential in the caudate (p = 0.26) and putamen (p = 0.12).

Table 1

In vitro binding data and intrinsic activity (IA) for compound **SV-III-130**.[a,b]

D_{2long}	D_3	D_4	D_2:D_3 Ratio	%IA D_2	%IA D_3
0.22 ± 0.01 nM	13.1 ± 2.3 nM	212 ± 45 nM	60	61.2 ± 4.4	52.5 ± 4.4

[a] K_i values (nM) were determined using human receptors expressed in HEK cells with ^{125}I-IABN. The K_i values represent the mean values for n > 3 determinations.

[b] Percent intrinsic activity (%IA) at human D2 or D3 receptors was determined using a forskolin-dependent adenylyl cyclase whole cell assay at a concentration of test compound >10 × K_i value. The mean values (n > 3) were normalized to values obtained using the full agonist quinpirole.

Table 2

Percent parent compound [^{11}C]**SV-III-130** in arterial blood samples of rhesus monkey

Time (min)	% Parent Compound
5	76.3 ± 1.7
30	60.6 ± 5.8

Table 3

DVR-1 and dopamine occupancy (DA OCC) induced by d-amphetamine in monkey caudate and putamen measured using [11C]**SV-III-130**.

Monkey[a]	Caudate DVR-1			Putamen DVR-1		
	Baseline[b]	AMPH[c]	DA[d] OCC	Baseline[b]	AMPH[c]	DA[d] OCC
Monkey 1	1.55	1.17	25%	1.70	1.45	15%
Monkey 2	1.80	1.05	42%	2.00	1.73	13%
Monkey 3	1.69	1.03	39%	1.85	1.22	34%
Monkey 4	1.71	1.43	16%	1.89	1.76	7%

[a]Four rhesus male monkeys were studied separately;

[b]Baseline DVR-1 values represent test-retest average of at least two studies for each individual monkey;

[c]D-amphetamine (AMPH) (1 mg/kg/i.v.) significantly decreased [11C]**SV-III-130** binding potential in striatal regions: caudate (p = 0.001) and putamen (p = 0.03);

[d]Percent dopamine (DA) occupancy (OCC) is higher in the caudate than in the putamen for all 4 monkeys.